is not sufficiently sedated. It is noteworthy that persistent bradycardia was observed by both CSM and HSF, and that the responses disappeared almost simultaneously in both tests. This correlation has not been previously reported.

In conclusion, we believe that more studies are needed to evaluate both the long-term efficacy of endocardial denervation of GP in patients with carotid syncope and the prognostic value of CSM responses as a target for neutralization during the procedure.

FUNDING

The publication of this clinical report is part of a research project funded by a grant from the *Asociación del Ritmo Cardiaco de la Sociedad Española de Cardiología* for postresidency research training in Spanish hospitals.

AUTHORS' CONTRIBUTIONS

C. Minguito Carazo and M. Rodríguez Mañero prepared and drafted the manuscript. All the authors were involved in the case and contributed to the revision and submission of the manuscript.

CONFLICTS OF INTEREST

None.

Carlos Minguito-Carazo,[a,b,*] Moisés Rodríguez-Mañero,[a,b,c] Jesús Martínez-Alday,[d] José Luis Martínez-Sande,[a,b,c] Laila González-Melchor,[a,b] and José Ramón González-Juanatey[a,b,c]

[a]*Unidad de Arritmias, Servicio de Cardiología y Unidad de Cuidados Intensivos Cardiológicos, Hospital Clínico Universitario de Santiago de Compostela, Santiago de Compostela, A Coruña, Spain*
[b]*Instituto de Investigación Sanitaria (IDIS), Universidad de Santiago de Compostela, Santiago de Compostela, A Coruña, Spain*
[c]*Centro de Investigación Biomédica en Red de Enfermedades Cardiovasculares (CIBERCV), Spain*
[d]*Unidad de Arritmias, Servicio de Cardiología, Hospital de Basurto, Bilbao, Vizcaya, Spain*

*Corresponding autor.
E-mail address: carlosminguito@hotmail.es (C. Minguito-Carazo).

Available online 15 June 2022

REFERENCES

1. Aksu T, Guler TE, Yalin K, Mutluer FO, Ozcan KS, Calò L. Catheter ablation of bradyarrhythmia: from the beginning to the future. *Am J Med Sci.* 2018;355:252–265.
2. Pachon MJC, Pachon EIM, Cunha Pachon MZ, et al. Catheter ablation of severe neurally meditated reflex (neurocardiogenic or vasovagal) syncope: cardioneuroablation long-term results. *Europace.* 2011;13:1231–1242.
3. Debruyne P, Rossenbacker T, Colliene C, et al. Unifocal right-sided ablation treatment for neurally mediated syncope and functional sinus node dysfunction under computed tomographic guidance. *Circ Arrhythm Electrophysiol.* 2018;11:e006604.
4. Palamà Z, Ruvo E, Grieco D, Borrelli A, Sciarra L, Calò L. Carotid sinus hypersensitivity syncope: is there a possible alternative approach to pacemaker implantation in young patients? *Postepy Kardiol Interwencyjnej.* 2017;13:184–185.
5. Brignole M, Groppelli A, Brambilla R, et al. Plasma adenosine and neurally mediated syncope: ready for clinical use. *Europace.* 2020;22:847–853.

https://doi.org/10.1016/j.rec.2022.04.015
1885-5857/

Thrombus discrimination using quantitative assessment of late-enhancement iodine maps and low monoenergetic imaging

Discriminación de trombos mediante evaluación cuantitativa de mapas de yodo e imágenes monoenergéticas de baja energía en realce tardío

To the Editor,

In the past decade, spectral computed tomography (CT) has emerged as a useful means to improve tissue characterization. However, few studies have explored its potential usefulness for the detection of cardiac and aortic thrombi.[1–3] Furthermore, although delayed-phase imaging typically provides the most valuable datasets aimed at ruling out thrombi, there are scarce reports regarding threshold values for thrombotic sources.[4] With the advent of dual-layer scanners that enable spectral routine acquisitions without protocol modifications, and in the context of acute ischemic stroke imaging, there is an expected increase in the number of scans with incidental thrombi. These scanners enable the availability of simultaneous multiparametric data including conventional CT images, monoenergetic imaging ranging from low (40keV) to high (200 keV) energy levels, and iodine density maps among others. Accordingly, we sought to evaluate the incremental value of monoenergetic and iodine density maps over conventional CT for the discrimination of thrombi in patients with acute ischemic stroke (AIS).

From July 2020, patients with suspected AIS admitted in our emergency department underwent a low-dose chest CT after CT angiography with the main goal of attempting to simultaneously rule out cardiovascular thrombotic complications using a dual-layer spectral CT (IQon Spectral CT, Philips Medical Systems Netherland B.V.). Low radiation dose chest CT (64 x 0.625 mm; voltage 120 kV; current 70-140 mA; gantry speed 270 ms; pitch 1.23; slice thickness 2.0 mm) was performed 5 minutes after contrast injection. Since all patients with suspected AIS undergoing CT are quantitatively assessed online using automated software (RAPID, iSchemaView, Menlo Park, USA), a process that takes between 5 and 10 minutes after contrast administration, delayed-enhancement spectral CT does not delay endovascular therapy.

All images were analyzed offline using dedicated software (IntelliSpace Portal version 11.1; Philips Medical Systems, Netherland B.V.) by a cardiovascular imaging expert with experience in dual energy cardiac CT blinded to the clinical history. Thrombi was defined as an abrupt focal filling defect with absent or nonsignificant contrast enhancement, clearly discriminated from surrounding structures such as blood and myocardial or vessel walls (figure 1).[1,5] Regions of interest (ROI) were adjusted to the size of the thrombi, with special care taken to avoid adjacent structures. An ROI was placed at the ascending aorta, enabling the assessment of the thrombi/aortic ratio, with the lowest values reflecting the largest differences. Images were evaluated using conventional CT

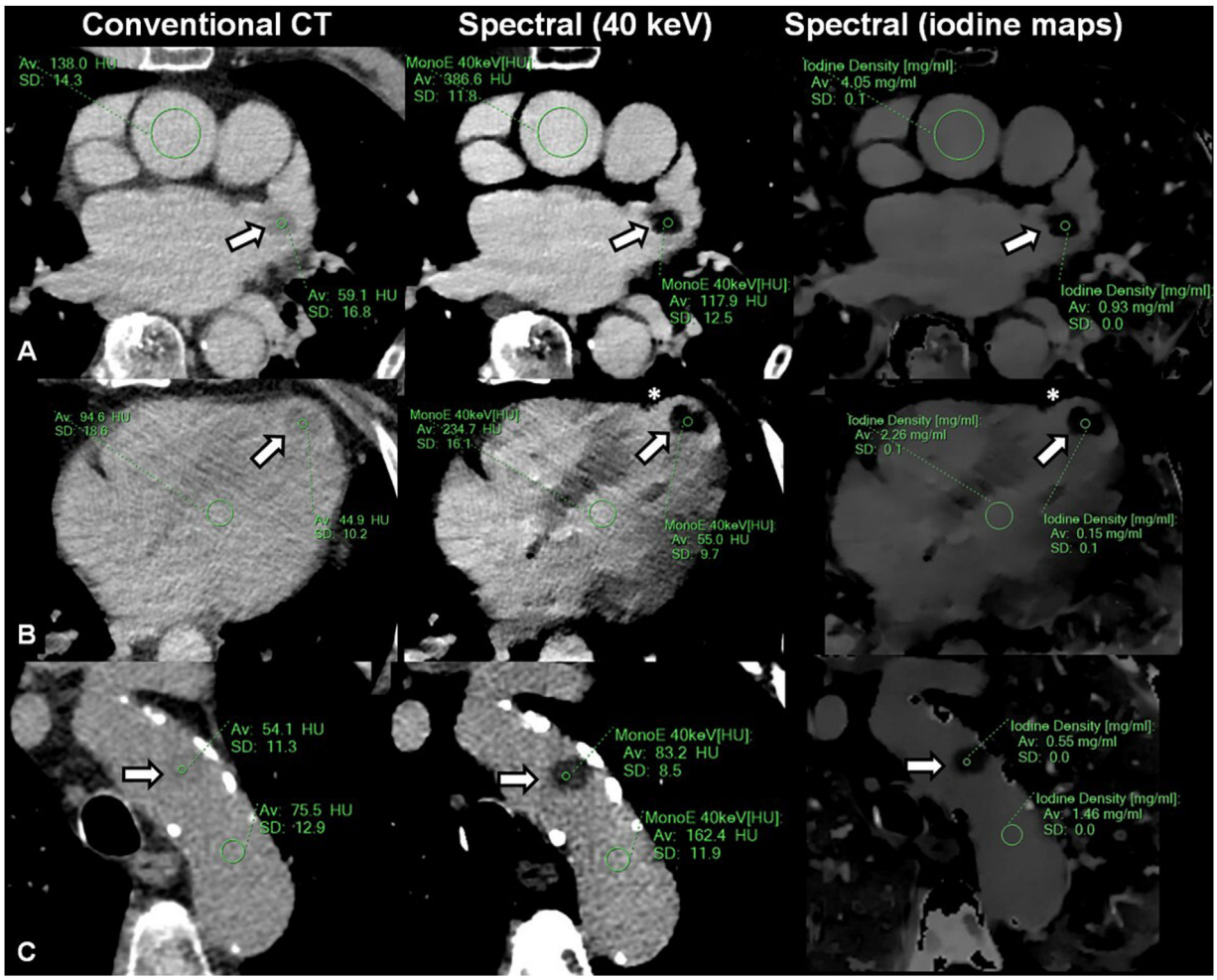

Figure 1. Patients with left atrial appendage (A), left ventricular (B), and aortic arch (C) thrombi evaluated using delayed-enhancement, low-dose, nongated, chest spectral computed tomography (CT) scans (delayed-enhancement spectral CT). Note that relatively vague differences using conventional CT (left panels) are more clearly discriminated by means of low monoenergetic (middle panels) and iodine density (right panels) imaging. Regions of interest (showing mean and standard deviation Hounsfield units [HU] and iodine densities) are deployed involving thrombi (arrows) and blood pool. Asterisks in panels B denote the presence of underlying myocardial infarction.

(Hounsfield units), monoenergetic imaging (Hounsfield units), at 40 keV, 55 keV, 70 keV, and 110 keV, and iodine-based results (mg/mL).

All participants provided written informed consent (habeas data) and this observational registry was approved by the institutional review board. The data supporting the findings of this study are available upon reasonable request.

From July 2020 to December 2021, 477 patients were admitted with an AIS. Of these, a cardiac or aortic thrombi was identified in 16 patients by using delayed-enhancement spectral CT. The mean age was 72.9 ± 13.3 years, with a mean baseline National Institutes of Health Stroke Scale of 13.0 ± 8.0. Six patients had atrial fibrillation and 6 had a history of coronary artery disease. All patients underwent transthoracic echocardiography during hospitalization, whereas 8 underwent advanced imaging with transesophageal echo or cardiac CT. Thrombi location comprised the left atrial appendage (LAA) in 6 patients, the left ventricle in 7 patients, and the aortic arch in 3 patients (figure 1). Although conventional CT yielded significant differences between the ascending aorta (blood) and thrombi (103.6 ± 18.3 HU vs 44.7 ± 13.7 HU; $P < .0001$), the largest differences were found using low monoenergetic imaging (40 keV = 265.2 ± 69.0 HU vs 69.0 ± 32.7 HU, $P < .0001$; 55 keV = 156.4 ± 36.0 HU vs 53.3 ± 19.2 HU, $P < .0001$; 70 keV = 107.0 ± 20.7 HU vs 46.3 ± 13.7 HU, $P < .0001$; 110 keV = 63.2 ± 8.3 HU vs 40.0 ± 10.0 HU, $P < .0001$) and iodine density maps (2.64 ± 0.8 mg/mL vs 0.38 ± 0.3 mg/mL; $P < .0001$) (table 1). The thrombi/aortic ratio were lower using iodine maps [conventional = 0.44 ± 0.16, 40 keV = 0.27 ± 0.13, 55 keV = 0.36 ± 0.14, 70 keV = 0.44 ± 0.16, 110 keV = 0.65 ± 0.19, iodine content = 0.15 ± 0.12, P (ANOVA) < .0001]. Compared with other locations, LAA thrombi showed the highest iodine content (left ventricle 0.21 ± 0.18 mg/mL vs LAA 0.89 ± 0.62 mg/mL vs aortic 0.18 ± 0.14, mg/mL; $P = .045$).

We demonstrated improved thrombi discrimination using spectral CT compared with conventional CT, with low energy monoenergetic imaging (40 keV) and iodine density maps showing the largest differences between thrombi and blood. Furthermore, we found variable iodine content according to the thrombus location and age, with LAA thrombi showing the highest iodine content compared with other locations. Accordingly, determination of single threshold values for the identification of thrombi might be inaccurate and should be specifically addressed in larger studies.[6] The relatively small number of thrombi involved might lead to selection bias and influence comparative analysis according to location. In addition, given the reassuring images as shown, confirmation with advanced imaging was considered redundant in some patients.

Table 1
Summary findings of density values (Hounsfield units), monoenergetic imaging (Hounsfield units) at increasing energy levels, and iodine-based results measured at the thrombotic source and at the ascending aorta

	Conv (HU)	Monoenergetic (HU)				Iodine (mg/mL)	ANOVA
		40 keV	55 keV	70 keV	110 keV		
Aorta	103.6 ± 18.3	265.2 ± 69.0	156.4 ± 36.0	107.0 ± 20.7	63.2 ± 8.3	2.64 ± 0.8	
Thrombi	44.7 ± 13.7	69.0 ± 32.7	53.3 ± 19.2	46.3 ± 13.7	40.0 ± 10.0	0.38 ± 0.3	
P value	< .0001	< .0001	< .0001	< .0001	< .0001	< .0001	
Thrombi/aorta	0.44 ± 0.16	0.27 ± 0.13	0.36 ± 0.14	0.44 ± 0.16	0.65 ± 0.19	0.15 ± 0.12	< .0001

Conv, conventional; HU, Hounsfield units; ANOVA, 1-way analysis of variance.

AUTHORS' CONTRIBUTIONS

Conception of the work, data analysis and interpretation, drafting, final approval, and assumption of responsibilities related to the content of the article: G.A. Rodríguez-Granillo. Design of the work, data collection, critical revision, final approval, and acceptance of responsibilities related to the content of the article: J. Cirio and Pedro Lylyk. Data collection, critical revision, final approval, and acceptance of responsibilities related to the content of the article: C. Bleise and L. Fontana.

FUNDING

No funding.

AUTHORS' CONTRIBUTIONS

Conception of the work, data analysis and interpretation, drafting, final approval, and assumption of responsibilities related to the content of the article: G.A. Rodríguez-Granillo. Design of the work, data collection, critical revision, final approval, and assumption of responsibilities related to the content of the article: J. Cirio and Pedro Lylyk. Data collection, critical revision, final approval, and assumption of responsibilities related to the content of the article: C. Bleise and L. Fontana.

CONFLICTS OF INTEREST

None of the authors has any conflicts of interest to declare related to the content of the manuscript.

Gastón A. Rodríguez-Granillo,[a,*] Juan J. Cirio,[b] Carlos Bleise,[c] Lucía Fontana,[a] and Pedro Lylyk[c]

[a]*Departamento de Imágenes Cardiovasculares, Instituto Medico ENERI, Clínica La Sagrada Familia, Buenos Aires, Argentina*
[b]*Unidad de Stroke, Instituto Medico ENERI, Clínica La Sagrada Familia, Buenos Aires, Argentina*
[c]*Departamento de Neurorradiología Intervencionista, Instituto Medico ENERI, Clínica La Sagrada Familia, Buenos Aires, Argentina*

* Corresponding author.
E-mail address: grodriguezgranillo@gmail.com
(G.A. Rodríguez-Granillo).
@eneri_neuro

Available online 1 June 2022

REFERENCES

1. Li W, Yu F, Zhu W, Zhang W, Jiang T. Detection of left atrial appendage thrombi by third-generation dual-source dual-energy CT: Iodine concentration versus conventional enhancement measurements. *Int J Cardiol.* 2019;292:265–270.
2. He YQ, Liu L, Zhang MC, Zeng H, Yang P. Dual-Energy Computed Tomography-Enabled Material Separation in Diagnosing Left Atrial Appendage Thrombus. *Texas Heart Inst J.* 2019;46:107–114.
3. Rodriguez-Granillo GA, Cirio JJ, Ciardi C, et al. Early Triage of Cardioembolic Sources Using Chest Spectral Computed Tomography in Acute Ischemic Stroke. *J Stroke Cerebrovasc Dis.* 2021;30:105731.
4. Romero J, Husain SA, Kelesidis I, Sanz J, Medina HM, Garcia MJ. Detection of left atrial appendage thrombus by cardiac computed tomography in patients with atrial fibrillation: a meta-analysis. *Circ Cardiovascular Imaging.* 2013;6:185–194.
5. Hur J, Kim YJ, Lee HJ, et al. Cardioembolic stroke: dual-energy cardiac CT for differentiation of left atrial appendage thrombus and circulatory stasis. *Radiology.* 2012;263:688–695.
6. Boodt N, Compagne KCJ, Dutra BG, et al. Stroke Etiology and Thrombus Computed Tomography Characteristics in Patients With Acute Ischemic Stroke: A MR CLEAN Registry Substudy. *Stroke.* 2020;51:1727–1735.

https://doi.org/10.1016/j.rec.2022.05.008
1885-5857/

Cardiac remodeling in patients with Marfan syndrome: impact of gender and vasodilator therapy

Remodelado cardiaco asociado con el síndrome de Marfan: impacto del sexo y el tratamiento vasodilatador

To the Editor,

Marfan syndrome (MS) is caused by a fibrillin-1 mutation, a component of the aorta and regulator of the signaling pathway of transforming growth factor beta. The aim of prescribing medications is to reduce the effects of fibrosis and blood pressure (BP) and prevent aortic dissection. Recent data support the existence of myocardial involvement in the presence of valves with normal function. Pathological myocardial remodeling is seen in the form of hypertrophy or dilatation, fibrosis, and left ventricular dysfunction. Systolic dysfunction occasionally remains subclinical and is only detected on myocardial strain measurement.[1] Postsystolic thickening (PST), which can be detected on echocardiography, has been described in states of pressure overload or myocardial ischemia.[1] The recently described high prevalence of PST among patients with MS even when BP is within normal limits indicates that the cardiomyopathy of MS has characteristics similar to states of pressure overload.[2]